INSTITUTE OF PHYSICS PUBLISHING PHYSICS IN MEDICINE AND BIOLOGY

Phys. Med. Biol. **52** (2007) 463–478 doi:10.1088/0031-9155/52/2/011

Laser-assisted cryosurgery of prostate: numerical study

Ricardo Romero-Méndez[1,2], **Walfre Franco**[1] **and Guillermo Aguilar**[1]

[1] Department of Mechanical Engineering, University of California, Riverside, CA 92521, USA
[2] Facultad de Ingeniería, Universidad Autónoma de San Luis Potosí, SLP, México 78290, Mexico

E-mail: gaguilar@engr.ucr.edu

Received 28 December 2005, in final form 20 September 2006
Published 29 December 2006
Online at stacks.iop.org/PMB/52/463

Abstract

A new methodology for preventing freezing damage beyond pre-specified boundaries during prostate cryosurgery is proposed herein. It consists of emitting controlled laser irradiation from the urethra, across the wall and into the prostate while conventional cryoprobes freeze the unwanted prostate tissue. The purpose of this methodology is to protect the urethral wall better and confine the desired cryoinjured region more accurately than the current cryosurgery approach. We also explore the potential use of light-absorbing dyes to further enhance the laser light absorption and corresponding heat generation to increase the thickness of the protected region. A finite difference heat diffusion model in polar coordinates with temperature-dependent thermophysical properties simulates the prostate freezing while laser irradiation across the urethral wall is emitted. This approach maintains the temperature of the urethral wall and the adjacent tissue above a pre-specified threshold temperature of -45 °C, independent of application time. Temperature contours resulting from prostate cryoablation with (a) conventional constant temperature heating; (b) laser irradiation heating; and (c) laser irradiation heating with pre-injected light-absorbing dye layers indicate that the thickness of the protected region increases in this order, and that the latter two methodologies may be more effective in limiting cryoinjury to a predefined region compared to constant temperature heating. An analysis of laser power requirements and sensibility of laser-assisted cryosurgery (LAC) of prostate is also presented. It is shown that tissue temperature may vary as much as ± 20 °C with variations of $\pm 10\%$ in laser power relative to the nominal power required to maintain the tissue at 37 °C. This demonstrates the sensitivity to laser power and the need of an accurate laser power control algorithm.

Nomenclature

C volumetric specific heat (J m^{-3} K^{-1})

E enthalpy (J)
f specular reflectance coefficient
h heat transfer coefficient (W m^{-2} K^{-1})
I_o laser flux density at surface of urethra (W m^{-2})
k thermal conductivity (W m^{-1} K^{-1})
L latent heat of fusion (J kg^{-1})
P laser power (W)
q heat flux (W m^{-2})
Q volumetric heat generation (W m^{-3})
r radial coordinate (m)
S surface
t time (s)
T temperature (°C)
V volume
w_{bl} blood perfusion rate (s^{-1})

Greek letters

δ_d thickness of dye layer (m)
μ_a absorption coefficient (m^{-1})
μ_s' reduced scattering coefficient (m^{-1})
μ_t' reduced total attenuation coefficient (m^{-1})
ϕ total light fluence (W m^{-2})
ϕ_C collimated light fluence (W m^{-2})
ϕ_D diffuse light fluence (W m^{-2})
θ angular coordinate

Subscripts

bl blood
bd body
c cryoprobe
d dye
i inner
l laser irradiation
met metabolic
nb neighbouring
nom nominal
o outer
p probe

Introduction

Cryoablation is a commonly used technique for the treatment of some types of cancer (Cohen *et al* 1998, Lee *et al* 1999, Stephenson 1999, Rees *et al* 2004). The concept, consisting of freezing tissue through the use of a solution of crushed ice and sodium chloride, was first proposed by Arnott (Arnott 1851, referenced by Rubinsky 2000), but the first cryosurgical device was developed by Cooper and Lee (Cooper and Lee 1961) in 1961. Cryoablation compares favourably with other techniques, such as radical surgery and irradiation of tissue

because it is less traumatic and reduces blood loss and hospitalization times (Holistic Urology 2006). It is the most recommended technique for patients who are too ill or too old to undergo major surgery, and for those with localized disease. Although used for various tissue malignancies, a very successful application of cryosurgery has been the eradication of prostate cancer. In 1993, Onik *et al* (1993) presented preliminary results indicating that ultrasound-guided prostate cryosurgery may be an effective treatment for prostate cancer.

During prostate cancer cryosurgery, cryoprobes consisting of a pair of concentric metal tubes (Chang *et al* 1994, Rabin and Shitzer 1996) of small diameter (through which cryogen flows) are inserted within the prostate. Freezing starts as the probes are turned on, and ice balls produced by each probe end up coalescing to form a larger one. The border of the large ice ball is monitored with the aid of transrectal ultrasound to ensure that it does not approach healthy tissue which, if damaged, would produce postoperative complications (e.g. urinary rectal fistula and urethral sloughing) hindering the success of the cryosurgical procedure.

To date, the success of cryosurgery for the eradication of prostate cancer is still very dependent on the experience and good judgment of the surgeon, who monitors and determines the growth of the ice ball (Mala *et al* 2004). To eliminate the intrinsic human error, the urethral wall may be protected from damage through the use of a urethral warmer, first proposed by Cohen *et al* (1995). Also, other investigations (Rabin and Stahovich 2002, 2003) have proposed the use of so-called cryoheaters, which are devices that use an electrical resistance to warm the urethral surface. The surgeon may also resort to treatment planning strategies, such as the optimal placement of cryoprobes to maximize ablation of the prostate while minimizing collateral damage. Studies aimed at improving cryoprocedures by numerically modelling the freezing and assessing the best placement for the cryoprobes have been carried out recently by other researchers; e.g. Baissalov *et al* (2001), Rewcastle *et al* (2001) and Rabin *et al* (2004).

In order to further increase the likelihood of a successful cryosurgery, it would be desirable to protect regions of healthy tissue without limiting the cryoablation of unwanted tissue so severely. If temperatures are maintained above the damage threshold within healthy tissue, independent of the cooling application time, great progress would be achieved. It is in this context that a preliminary investigation on the use of laser irradiation for tissue protection during cryosurgery, referred to as laser-assisted cryosurgery (LAC), was recently proposed by Romero-Mendez *et al* (2005) for the case of a simple geometry. The present investigation compares the protective effect achieved by LAC to that obtained by more conventional means of heating, such as warmers and cryoheaters, for the case of prostate cryosurgery.

Problem description

Laser irradiation to protect the urethral wall can be achieved using a system such as that represented in figure 1. A laser fibre is introduced via a catheter inside the urethra, with saline water solution circulated through it to prevent overheating. Cryoprobes are then inserted around the urethra. The cryoprocedure starts by turning the cryoprobes on to initiate the freezing process, followed by laser heating aimed at the region around the urethra including its wall. As a consequence of this heating, the freezing front is stopped at some distance from the urethral wall and a steady state temperature distribution is reached in its neighbourhood.

The objective of the present study is to assess the advantages that regulated *laser irradiation heating* of LAC may have over *constant temperature heating* for protecting the urethral wall and surrounding tissue during cryosurgery. In this context, we define 'protected region' as the region of tissue that is maintained at or above a lethal temperature, T_{lethal}, of $-45\ ^{\circ}\text{C}$, in accordance with Rabin and Stahovich (2002), who considered $-45\ ^{\circ}\text{C}$ as the temperature that guarantees cell death of urethral and prostatic tissue.

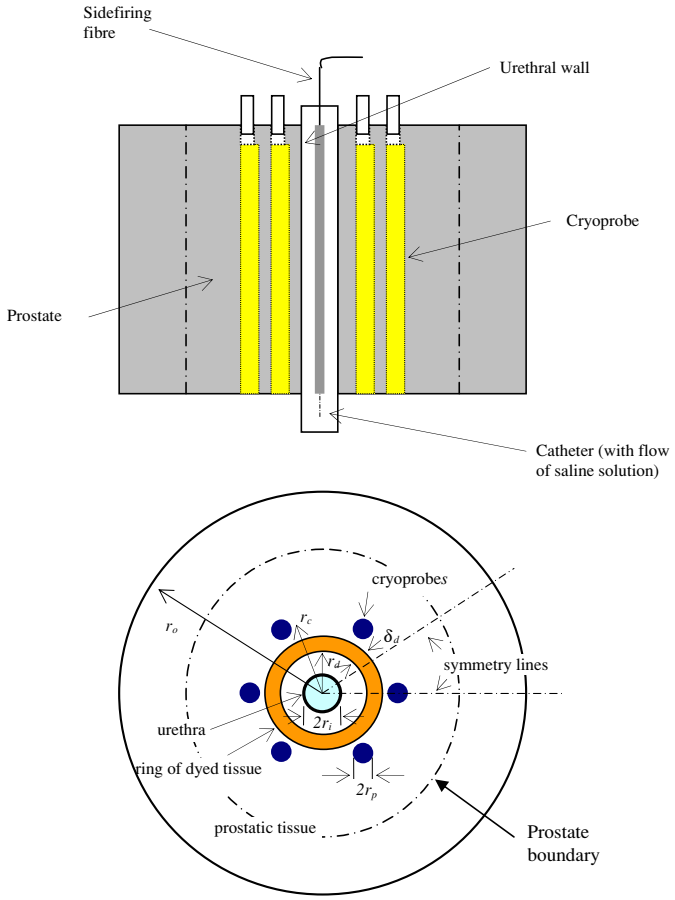

Figure 1. Intra-urethral laser irradiation of prostate during cryosurgery.
(This figure is in colour only in the electronic version)

The region to be analysed (figure 1) is the annulus of inner radius r_i and outer radius r_o, representing the prostate and surrounding tissue. Inside this domain, six cryoprobes, each of outer radius r_p and with a surface temperature T_c, are placed and evenly distributed at a distance r_c from the centre. The heating device is contained within the urethral tube, which is represented by the inner circle of radius r_i.

Mathematical formulation

The energy equation during the cryosurgical procedure is represented mathematically by the bio-heat equation (Pennes 1948):

$$\nabla \cdot (k \nabla T) + Q_l + w_{bl} C_{bl} (T_{bl} - T) + Q_{\text{met}} = C \frac{\partial T}{\partial t}, \tag{1}$$

where k is the thermal conductivity, T is the temperature, Q_l is an internal heat source term due to absorption of laser energy, w_{bl} is the blood perfusion rate, C_{bl} is the volumetric specific heat of blood, T_{bl} is the blood temperature (typically the body temperature), Q_{met} is the metabolic heat generation, C is the volumetric specific heat of tissue and t is the time.

As explained by Rabin and Stahovich (2003), equation (1) is suitable for representing heat flow in the presence of dense capillary networks and not in the presence of major blood vessels. However, newer models involve greater mathematical complexity without necessarily adding higher accuracy. Therefore, for a proof of principle study like this, the classical bioheat equation used herein is an appropriate choice.

The tissue is initially at body temperature T_{bd}. The cryoprobes are assumed to have a surface temperature T_c. The ratio of the outer to inner radii, r_o/r_i, is large enough and the cryoprobes are located much closer to the inner circle of radius r_i, such that for sufficiently short times, the initial temperature at the boundary, $r = r_o$, is assumed to be unaffected. The boundaries $\theta = 0$ and $\theta = \pi/6$ are symmetry planes; zero heat flux boundary conditions are established therein. At the heating boundary, $r = r_i$, three different conditions are established depending on how heat is being applied:

(a) *Constant temperature heating*. The urethral tube is assumed to be in perfect thermal contact with the catheter surface at T_{bd}; that is, $T(r_i, \theta) = T_{bd}$.

(b) *Laser irradiation heating*. The urethral surface experiences forced heat convection with the circulating saline solution at T_{bd} and the associated convective heat transfer coefficient, h, thus

$$-k\frac{\partial T}{\partial r}\bigg|_{r=r_i} = h\big(T|_{r=r_i} - T_{bd}\big). \tag{2}$$

The heat source term $Q_l(r)$ that represents energy absorption within tissue is written as

$$Q_l(r, \theta) = \mu_{a,j}\phi_j(r, \theta), \qquad r_i \leqslant r \leqslant r_o, \qquad 0 \leqslant \theta \leqslant 2\pi, \tag{3}$$

where $\mu_{a,j}$ is the tissue optical absorption coefficient, and ϕ_j is the total light fluence at r. ϕ_j is the sum of the collimated light $\phi_{C,j}$ and the diffuse light $\phi_{D,j}$:

$$\phi_j(r, \theta) = \phi_{C,j}(r, \theta) + \phi_{D,j}(r, \theta), \tag{4}$$

where r and θ are the radial and angular coordinates, and the subindex j denotes either normal (no subindex) or dyed tissue (replacing j for d). $\phi_{C,j}$ is defined as

$$\phi_{C,j} = I_{o,j}\frac{r_{i,j}}{r}(1 - f)\exp[-\mu'_{t,j}(r - r_{i,j})], \tag{5}$$

where $I_{o,j}$ is the flux density incident at every new layer of tissue that starts at $r_{i,j}$. In the case of the first layer, $I_{o,j}$ is directed normally through the catheter surface by a dispersing side-firing fibre located within the urethra. f is the specular reflectance coefficient and $\mu'_{t,j}$ is the total attenuation coefficient—defined as the sum of the absorption coefficient $\mu_{a,j}$ and the reduced scattering coefficient $\mu'_{s,j}$. $\phi_{D,j}$ is calculated from the steady-state optical diffusion equation

$$\nabla^2\phi_{D,j} - 3\mu_{a,j}\mu'_{t,j}\phi_{D,j} = -\frac{\mu'_{s,j}}{D_j}\phi_{C,j} \tag{6}$$

where the optical diffusion coefficient is $D_j = 1/3\mu'_{t,j}$. At the urethra surface an internal reflection factor A is introduced to consider the effect of mismatched boundaries, such that

$$\phi_{D,j} = 2AD_j\nabla\phi_{D,j}\cdot\vec{n}, \tag{7}$$

where $\vec{n}$ is the inward unit vector normal to the urethral surface. $A = (1 + a)/(1 - a)$, where $a = 0.49$ (Star 1995). At far distance from the urethral surface ($r \to \infty$) a zero fluence boundary condition is assumed:

$$\phi_{D,j}(\infty, \theta) = 0. \tag{8}$$

Table 1. Properties of prostate tissue according to Rabin and Stahovich (2003).

T (°C)	C (J m^{-3} K^{-1})	k (W m^{-1} K^{-1})	$w_b C_b$ (W m^{-3} K^{-1})	L (MJ m^{-3})
$T > 0$	3600	0.5	40×10^3	
$-22 \leqslant T \leqslant 0$	15 440	$15.98 + 5.67 \times 10^{-2}(T + 273)$	$40 \times 10^3\ (T + 22)/22$	300
$T < -22$	$7.57\ (T + 273)$	$1005\ (T + 273)^{-1.15}$	0	

The cryoprobes are not considered as light absorbers because they are inserted at a distance from the urethral wall much larger than the penetration depth ($1/\mu_t' \approx 0.7$ mm) of light in tissue at the simulated wavelength (710 nm).

To avoid undesirable heating damage, the laser fluence I_o is adjusted such that the maximum temperature within the tissue is T_{bd}. Concurrently, this allows us to compare the protecting effect of LAC versus condition (a), *constant temperature heating*. The minimum temperature is bound by T_{lethal}, which is especially important to monitor and avoid around the urethra. Since the propagation of the freezing front (and the T_{lethal} temperature front) during the transient process is always towards the heating surface, the worst case scenario for tissue freezing damage is when the steady state temperature is reached around the urethra, which is when the freezing front approaches the heating boundary.

(c) *Laser irradiation heating with pre-injected light-absorbing dye*. In order to determine how the potential use of high absorbing dyes might modify the temperature field within the tissue during laser irradiation, a dye that changes the absorption coefficient from μ_a to $\mu_{a,d}$ and keeps the same scattering coefficient as the regular tissue, $\mu_s' = \mu_{s,d}'$, is injected within the region surrounding the urethra at different radial positions, r_d (see figure 1). In order to keep the problem bounded, a single thickness of dye layer, δ_d, was used throughout the simulations.

The geometric dimensions (figure 1) used in this study are the following: $r_i = 2.5 \times 10^{-3}$ m; $r_p = 0.75 \times 10^{-3}$ m; $r_o = 40 \times 10^{-3}$ m; 6×10^{-3} m $< r_c < 20 \times 10^{-3}$ m; and $r_d = 8 \times 10^{-3}$ m. While a prostate may be approximated by a sphere with a radius of 25 mm (see figure 1), we chose a computational domain of 40 mm to represent the soft tissue adjacent to the prostate and to ensure that the temperature at such distance remains unchanged up to the maximum computation time used in this study (1200 s). The initial temperature of the tissue is $T_{bd} = 37$ °C. In the case of laser irradiation, the inner urethral wall ($r = r_i$) exchanges heat by convection with a fluid that circulates within the urethra at $T_{bd} = 37$ °C. The associated convective heat transfer coefficient is assumed to be $h = 250$ W m^{-2} K^{-1}, which is within the range of values of h expected for forced convection of a fluid circulating laminarly through a pipe (Incropera and DeWitt 2002). In any case, as corroborated by preliminary computations, the magnitude of h does not have a strong influence on the temperature variation within the region because laser irradiation is always adjusted to maintain the temperature of the urethral wall close to that of the circulating saline fluid, i.e., $T_{bd} = 37$ °C. Inserted inside the tissue is the cryoprobe that maintains a surface temperature of $T_c = -145$ °C, characteristic of cryoprobes that use the argon gas Joule–Thomson cooling effect (Rabin and Stahovich 2002).

The properties of the tissue are temperature dependent, and the liquid to solid phase change is taken into account by the specific heat value within a temperature range between 0 and −22 °C. The properties of C and k are represented according to the expressions shown in table 1, characteristic of soft biological tissues (Rabin and Stahovich 2002). The blood perfusion heating effect, $w_{bl}C_{bl}$, of soft biological tissues varies within the range 0 to 40 kW m^{-3} K^{-1} (Rabin and Stahovich 2002). Although blood circulation stops once the

tissue is frozen, the prostate is a well irrigated organ, thus $w_{bl}C_{bl}$ is given a range of values as described in table 1. Values $\mu_a = 37\ \mathrm{m}^{-1}$ and $\mu_s' = 1400\ \mathrm{m}^{-1}$ of prostate tissue are used, corresponding to a laser wavelength of 710 nm (Zhu *et al* 2005). The absorption coefficient of the dyed tissue is chosen to be $\mu_{a,d} = 500\ \mathrm{m}^{-1}$ and the reduced scattering coefficient of dyed tissue is kept at $\mu_{s,d}' = 1400\ \mathrm{m}^{-1}$.

Numerical solution of the problem

The Pennes bio-heat transfer equation is solved numerically by the enthalpy method (Alexiades and Solomon 1993) as follows:

$$\int_t^{t+\Delta t} \frac{\partial}{\partial t}\left(\int_V E\,\mathrm{d}V\right)\mathrm{d}t = \int_t^{t+\Delta t}\int_S -\vec{q}\cdot\vec{n}\,\mathrm{d}S\,\mathrm{d}t + \int_t^{t+\Delta t}\int_V Q\,\mathrm{d}V\,\mathrm{d}t, \tag{9}$$

which is the integral heat balance over a control volume and time-interval. E is the enthalpy per unit volume and $Q = Q_l + Q_{\mathrm{met}} + w_{bl}C_{bl}\left(T_{i,j}^n - T_{bl}\right)$ is the volumetric heat generation term. The numerical scheme used to solve equation (9) is based on an explicit finite volume formulation in polar coordinates:

$$E_{i,j}^{n+1} = E_{i,j}^n + \frac{\Delta t}{\Delta V}\sum_1^4 q_{nb} + \frac{\Delta t}{\Delta V}\int_{\theta_{\iota-\frac{1}{2}}}^{\theta_{\iota+\frac{1}{2}}}\int_{r_{j-\frac{1}{2}}}^{r_{j+\frac{1}{2}}} Q(r)r\,\mathrm{d}r\,\mathrm{d}\theta, \tag{10}$$

where $\Delta V = r\Delta r\Delta\theta$, and q_{nb} are the heat that flows through the four boundaries of the control volume i, j. The enthalpy term is related to temperature according to the following expressions obtained by substituting in $E_{i,j} = \int C\,\mathrm{d}T_{i,j}$ the values of C expressed in table 1:

$$E_{i,j}^n(x,y,t) = \begin{cases} 3.785\left(T_{i,j}^n\right)^2 + 2066.62T_{i,j}^n + 43\,632 & T_{i,j}^n \leqslant -22\ ^\circ\mathrm{C} \\ 15\,440T_{i,j}^n + 339\,680 & -22\ ^\circ\mathrm{C} < T_{i,j}^n < 0\ ^\circ\mathrm{C} \\ 3600T_{i,j}^n + 339\,680 & T_{i,j}^n \geqslant 0\ ^\circ\mathrm{C}. \end{cases} \tag{11}$$

The numerical simulation is performed in a mesh containing 20 by 100 divisions in the θ and r directions, respectively. A finer mesh is used in the region $r_i \leqslant r \leqslant r_c$ and gradually increases in size in the region $r_c \leqslant r \leqslant r_o$. The time interval is restricted by the stability criterion that applies to explicit finite volume formulations (Alexiades and Solomon 1993). In order to study the grid-independence of the results, a numerical simulation was run for a mesh containing 30 by 150 divisions in the θ and r directions, respectively, for the case $r_c = 1 \times 10^{-2}$ m. The difference in the final position of the T_{lethal} contour obtained between the two meshes was very small (less than 0.93%). Therefore we proceeded to compute our simulations with the 20 by 100 grid.

Equations (9) to (11) are solved numerically by means of a finite difference algorithm and the resulting set of algebraic equations is solved using the Thomas tri-diagonal algorithm (Press *et al* 1986).

Results

Validation

The numerical code used in this study was validated by comparing the results to those obtained by Rabin and Stahovich (2002) for a similar geometry and constant temperature heating of the urethral wall. Other models, although not necessarily for the same geometry, have been developed over the years, such as Cooper and Trezek (1972), Rewcastle *et al* (1998), Rubinsky and Pegg (1988) and more recently Liu *et al* (2004). However, we considered Rabin and

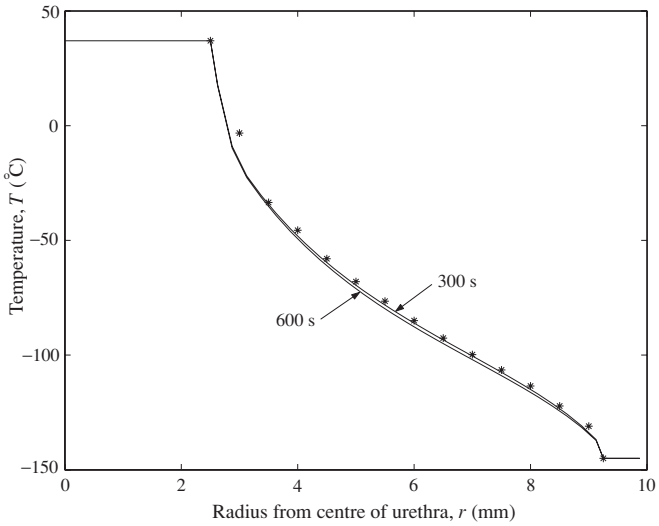

Figure 2. Temperature profiles, $T(r, 0)$, for the case of constant temperature heating. Comparison of results obtained in this investigation at two different simulation times ($t = 300$ s and 600 s) (—) and those by Rabin *et al* (2004) for $t = 600$ s (*).

Stahovich's results to validate our model because it is a recent study that focuses on the same application of our interest. The solid lines in figure 2 show the temperature profiles along the line $\theta = 0$, $r_i \leqslant r \leqslant (r_c - r_p)$ for the case $r_c = 10$ mm at two different times (300 and 600 s) superimposed on the simulations of Rabin and Stahovich (Rabin and Stahovich 2002) at 600 s, represented by symbols, showing a very good match.

There are two clearly defined regions in the computational domain: (i) the region between the heating surface and the cryoprobe ($r_i \leqslant r \leqslant r_c$), and (ii) the region beyond the cryoprobe ($r_c \leqslant r \leqslant r_o$). Figures 3(a) and (b) show the time dependence of temperature during *laser irradiation heating* along $\theta = 0$ and $\theta = \pi/6$, respectively, for $r_c = 10$ mm. Region (i) quickly evolves into a steady state temperature profile while the temperature profile in region (ii) changes more gradually. Note that the temperature profiles show an increase in the radius of influence of the cryoprobes as time progresses. Region (i) is the one of interest since it is the area near the urethral wall that must be protected by laser irradiation. Unless indicated otherwise, all numerical simulations are for $t = 600$ s, after which time the temperature profiles of region (i) do not change considerably, and those of region (ii) are evolving very slowly, displacing outwards the zone of influence of the cryoprobes.

Comparison of temperature profiles

In their figure 7, Rabin and Stahovich (2002) show the temperature profiles at $\theta = 0$ for *constant temperature heating*, and different positions of the cryoprobes, r_c. There is a steep temperature gradient near the urethral surface, $r_i = 2.5$ mm, and only a very thin layer around the urethra is above T_{lethal}. Figure 4 shows $T(r, 0)$ for *laser irradiation heating* at different cryoprobe positions (r_c). For this case, the layer of tissue above T_{lethal} (with a 3.12 mm thickness for the case of $r_c = 10$ mm) is larger than that of *constant temperature heating* (a 1.33 mm thickness in figure 7 of Rabin and Stahovich 2002). This is because laser light absorption and heat generation occurs over a tissue volume whose depth depends on the optical properties of the tissue, as opposed to contact heating where heat must propagate exclusively by conduction across the surface $r = r_i$.

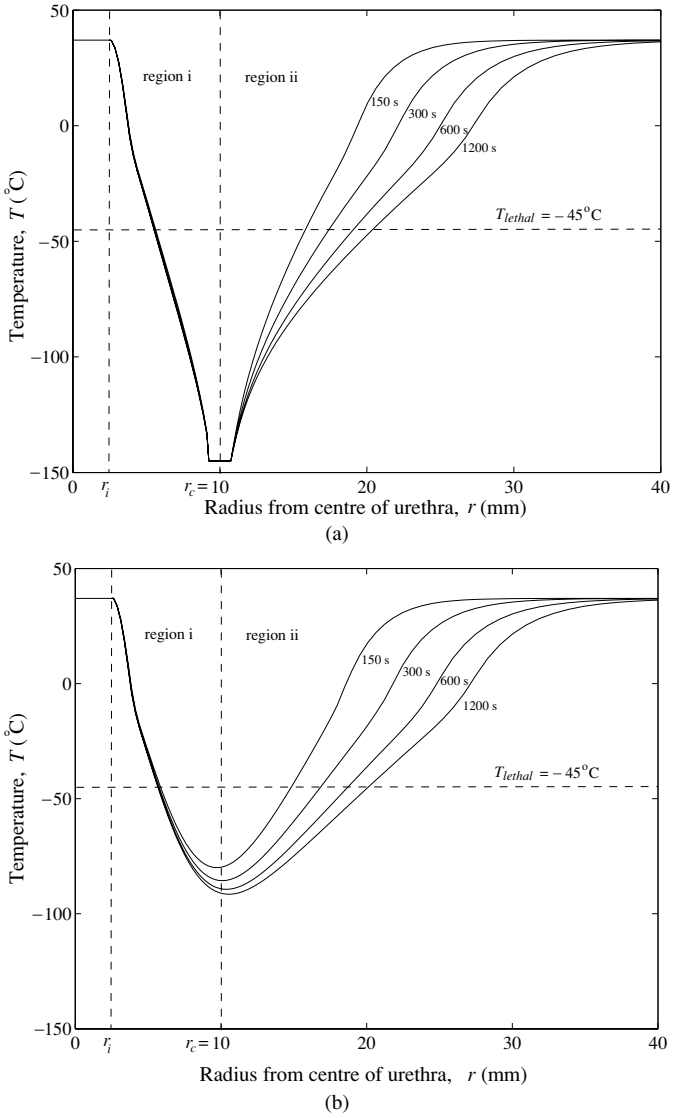

Figure 3. Temperature profiles at different times for the case of *laser irradiation heating*. Cryoprobe at $r_c = 10$ mm. (a) $T(r, 0)$, (b) $T(r, \pi/6)$.

Comparison of protection achieved by constant temperature, laser irradiation and laser irradiation plus dye heating

Figure 5 shows the average thickness of tissue that can be protected using the three heating methods for the cases of $\theta = 0$ and $\theta = \pi/6$. In the case of dyed tissue $r_d = 8$ mm and $\delta_d = 2$ mm. It can be seen that *laser irradiation heating* protects a layer of tissue at least 2.3 times thicker than that of *constant temperature heating*. Additionally, the imperfect thermal contact not considered in the simulations, but expected to occur between the cryoheater and urethral wall, may make this difference even larger. Furthermore, the hypothetical case of injection of a dye at a certain tissue depth would produce an extra benefit of absorbing most of the laser energy at selected regions inside the tissue. Thus, the T_{lethal} isotherm would be

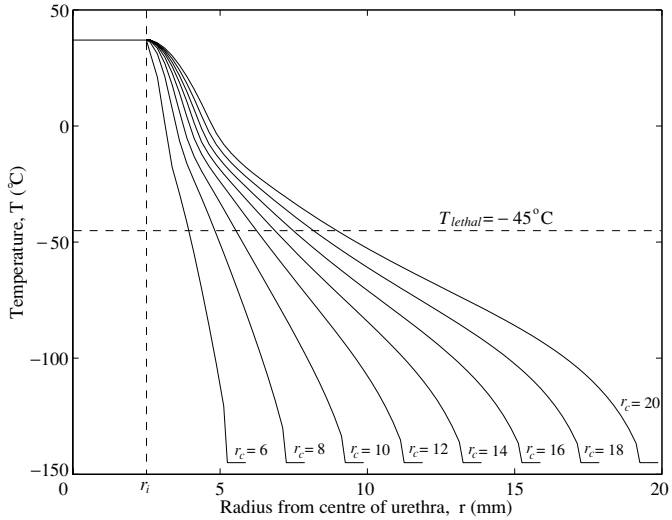

Figure 4. Temperature profiles, $T(r, 0)$, at $t = 600$ s for different values of r_c (expressed in mm). Cases of *laser irradiation heating*.

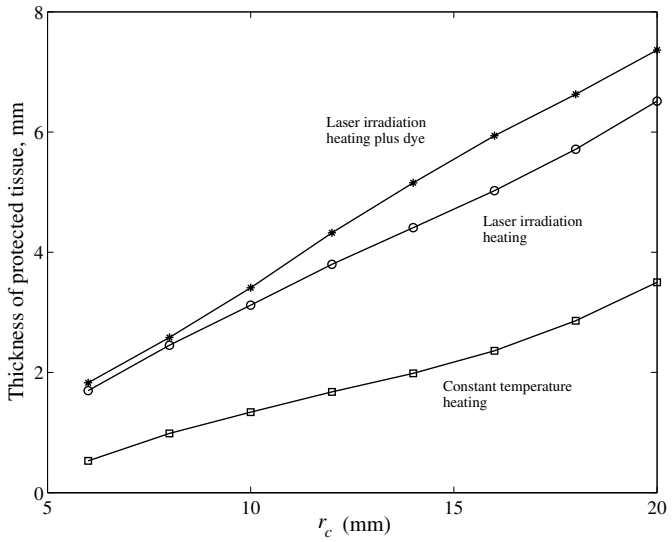

Figure 5. Average thickness of tissue protected by *constant temperature*, *laser irradiation heating* and *laser irradiation heating plus dye* for different cryoprobes positions.

displaced further from the urethral surface and, consequently, increase the thickness of the protected tissue. Note that for values of $r_c \leqslant r_d$ ($r_d = 8$ mm), the protection thickness for the *laser-induced heating* and *laser-induced heating plus dye* is almost the same because the dye ring is located closer to the centre than the cryoprobes, but as r_c increases, so does the protection obtained using dyes.

Laser power regulation

Of concern to the implementation of LAC is the power needed to achieve the desired protection. In order to avoid high temperatures, the energy must be regulated by pulsing the laser to control

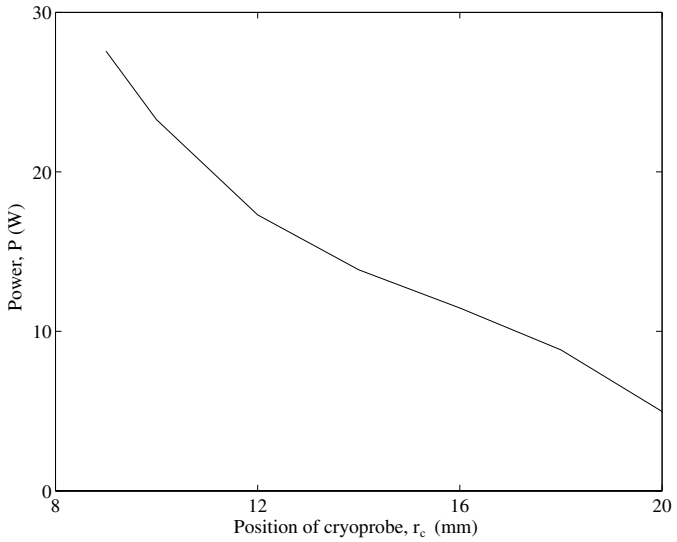

Figure 6. Steady state power required to regulate the temperature within the tissue such that $T_{\max} = 37\ ^{\circ}\mathrm{C}$. Power as a function of r_c.

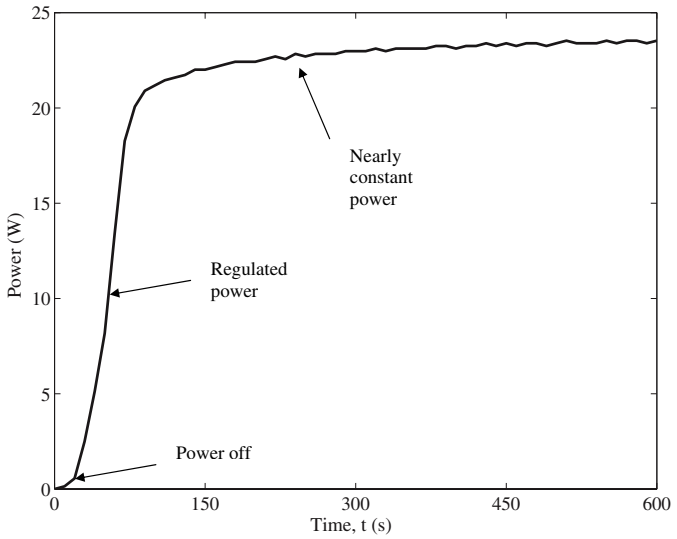

Figure 7. Laser power required to maintain the temperature within the tissue such that $T_{\max} = 37\ ^{\circ}\mathrm{C}$ when $r_c = 10$ mm. Power as a function of time.

the power. Figure 6 shows the laser power necessary to maintain the urethral 'protection' by avoiding temperatures above $T_{\max} = 37\ ^{\circ}\mathrm{C}$ within the tissue. The power increases as r_c decreases. This is because the temperature gradient is steeper when the cryoprobes are closer to the urethra and the laser power needed to exchange heat with the cryoprobes is larger.

Since the time scale for energy transport by conduction in tissue is different to that for laser energy absorption, the six cryoprobes and the laser must be turned on at different times and the laser energy must be supplied gradually during the procedure. Figure 7 shows the power that must be supplied by the laser as a function of time during a cryotherapy procedure

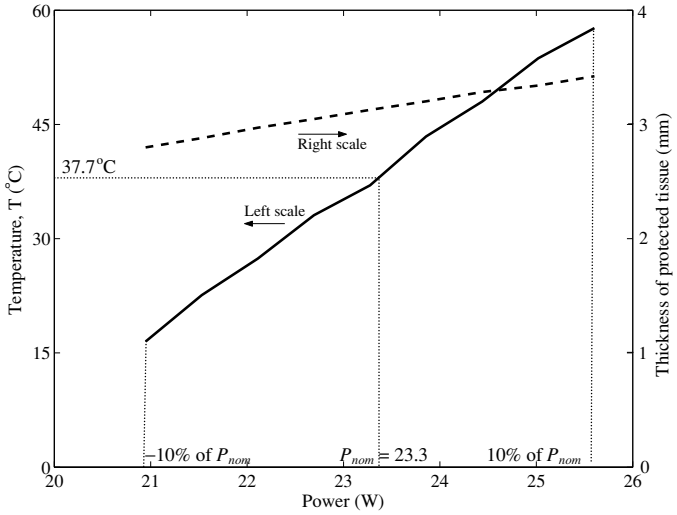

Figure 8. Maximum temperature (——) and thickness of protected tissue (– – –) as a function of laser steady state power supply for $r_c = 10$ mm.

in order to maintain the maximum temperature below 37 °C. Initially, the laser must stay off. Next, the power must be regulated to avoid excessive heating, and for later stages of the cryoprocedure, nearly continuous power must be supplied.

Laser power sensitivity

If the power supplied by the laser, P, differs from the nominal power, P_{nom}, required to maintain $T_{\max} = 37$ °C, $T_{\max}$ will vary and so will the position of the T_{lethal} isotherm. Figure 8 shows the maximum temperatures reached in the tissue as a function of P. As seen, the temperature is very sensitive to laser power, with a maximum temperature of 57.7 °C obtained when P is 10% higher than P_{nom} and a minimum of 16.5 °C when P is 10% lower than P_{nom}. Figure 8 also shows the position of T_{lethal} front as a function P. The thickness of the protected layer reduces by 11.9% when P is 10% lower than P_{nom}, but the protected thickness under those circumstances is still much larger than that obtained using *constant temperature heating* (as seen from figure 5).

Optical properties sensitivity

Another important consideration in the implementation of power control for LAC is the effect of optical property variations on overall tissue temperature and protection thickness. Figures 9(a) and (b) show the maximum temperature and thickness of protected tissue expected for a fixed $P_{\text{nom}} = 23.3$ W applied to tissues with different optical properties. Figures 9(a) and (b) show the effect of a variation of ±10% in the prostate *absorption* coefficient ($\mu_a = 37$ m^{-1}) and *reduced scattering* coefficient ($\mu_s' = 1400$ m^{-1}), respectively, on the maximum temperature and protection thickness. As seen, a variation of ±10% on both μ_a and μ_s' may induce a 30 °C variation on the maximum temperature and about 5.7% variation on the protection thickness. These are important considerations to be made during the planning of power control. It is important to note, however, that even if P_{nom} is reduced by 10% to prevent potential overheating due to uncertainty of the optical properties, the thickness of protected tissue obtained by *laser irradiation* would still be greater than that obtained by *constant temperature heating* (as seen from figure 5).

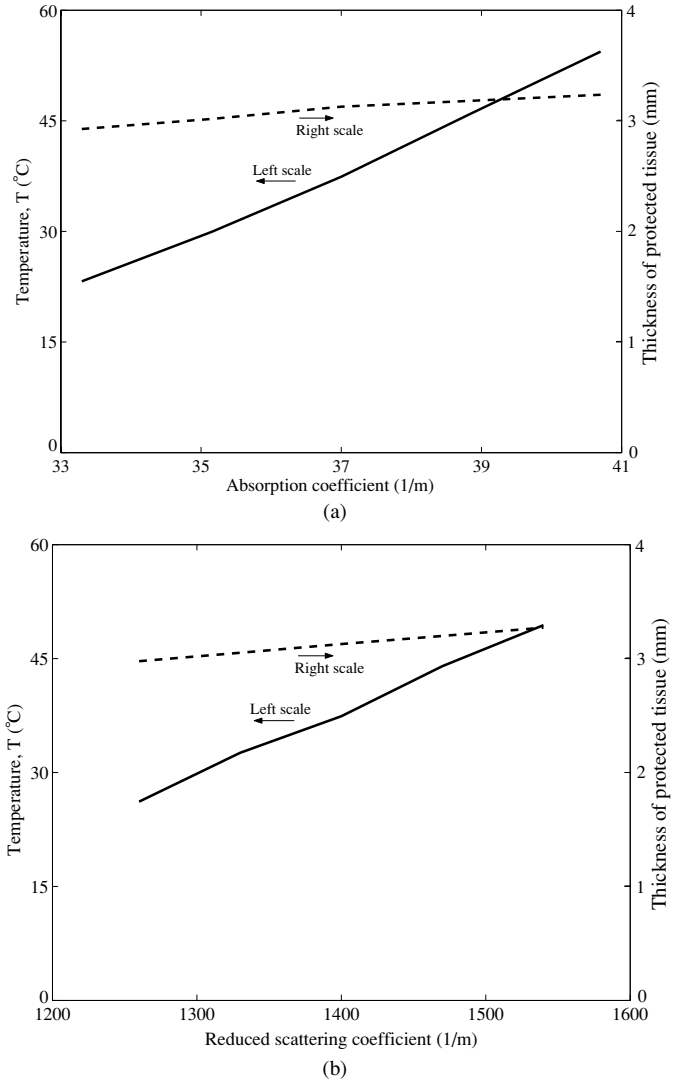

Figure 9. Maximum temperature (——) and thickness of protected tissue (– – –) as a function of tissue optical properties for a fixed laser power, $P_{\text{nom}} = 23.3$ W, and $r_c = 10$ mm. (a) Variation of absorption coefficient within $\pm 10\%$ of the value $\mu_a = 37\ \text{m}^{-1}$, (b) variation of reduced scattering coefficient within $\pm 10\%$ of the value $\mu_s' = 1400\ \text{m}^{-1}$.

We also note that μ_a and μ_s' are wavelength dependent. As such, the light distribution, penetration depth and resulting heat generation will depend on the laser of choice. For example, bulk heating (more convenient in the absence of dyes) may be more readily attainable with near infra-red wavelengths, while more selective heating (more convenient in the presence of dyes) may be possible with visible wavelengths. In any case, it is important to have proper estimates of what the spectral optical properties of prostate are.

The tissue optical properties are expected to change with temperature. In particular, frozen tissue is expected to have a higher scattering coefficient than fresh tissue, which reduces the light penetration depth but is dependent on the freezing speed. Conversely, the refractive

index of ice is smaller than that of water, which increases the light penetration depth and, thus, may compensate the effect of increased scattering. Studies of cryopreservation on the optical properties of human aorta have shown a decrease in μ_a by as much as 11% and an increase of up to 43% in μ_s' of thawed tissue as compared with fresh tissue (Çilesiz and Welch 1994). Hence, it is reasonable to consider at least three different sets of optical tissue properties as a function of the tissue state, namely, fresh, transition and frozen.

In this pilot study, we considered only optical properties of fresh tissue based on the discussion presented above and the fact that the absorption coefficients of ice and water at a similar wavelength (710 nm) are small and of the same order of magnitude: 0.03 m^{-1} (Hale and Querry 1973, Warren 1984).

Assuming a similar trend in changes in the optical properties in human prostate as those of human aorta, the penetration depth of light at the frozen state would be higher than the penetration depth at the transition state, which in turn would be higher than the penetration depth at the fresh state. In that case, light would penetrate farther than our model predicts.

Finally, improper balance between the tissue freezing and laser irradiation may lead to undesired thermal damage during LAC. It is customary to represent cumulative thermal damage within tissue, Ω, by a first-order kinetic model (Arrhenius integral):

$$\Omega = A \int_0^t \exp\left(-\frac{E_a}{RT(\tau)}\right) \mathrm{d}\tau, \tag{12}$$

where A is the frequency factor, E_a is the activation energy threshold, R (8.32 J $mole^{-1}$ K^{-1}) is the universal time constant (Henriques 1947) and $T(\tau)$ the time-dependent tissue temperature. Irreversible injury to tissue is assumed to occur when $\Omega = 1$, which represents denaturation of 63.2% $(1 - 1/e)$ of the native tissue. For such conditions and for bulk skin, $A = 3.1 \times 10^{98}$ s^{-1} and $E_a = 628 \times 10^3$ J $mole^{-1}$ (Henriques 1947), the critical temperature for bulk skin heating damage, T_c, is

$$T_c = \frac{E_a}{R \ln(A)} \approx 60\ ^\circ\mathrm{C}. \tag{13}$$

It is reasonable to expect a similar T_c for prostate. Therefore, considering that the power control for laser irradiation is intended to maintain tissue at or near normal body temperature ($T_{bd} = 37\ ^\circ$C) and that even the estimated 10% increase in P_{nom} due to the uncertainty in the optical properties would lead to a maximum temperature rise below T_c, thermal damage due to overheating seems an unlikely scenario. Nevertheless, reliable estimates of the thermal and optical properties of prostate and, most importantly, experimental confirmation of LAC are necessary steps that must be taken before this approach is even considered for pre-clinical and clinical trials.

Conclusions

The study presented herein explores the use of laser irradiation heating for confining the freezing front propagation during prostate cryosurgery, an approach we have referred to as laser-assisted cryosurgery (LAC). The present investigation compares the protective effect achieved by LAC to that obtained by more conventional means of heating, such as warmers and cryoheaters. For this purpose, a numerical simulation is performed, and (worst case scenario) thermal damage is computed for steady state conditions in the region around the urethra. The differences in thermal confinement produced by conventional constant temperature heating and laser irradiation are assessed. The results show that LAC achieved by *laser irradiation heating* protects a much thicker layer of tissue than *constant temperature heating*. Protection

may be further increased by dyes injected into the tissue to promote localized absorption of laser light. It is important to stress, however, that reducing the uncertainty in the selection of tissue properties by carrying out *in situ* measurements, the use of more precise bioheat models and, most importantly, the need for experimental confirmation are necessary steps that must be taken before the LAC approach may be even considered for pre-clinical and clinical trials.

The power needed to maintain the tissue at a specified maximum temperature must be determined for every particular LAC application, and it is a function of the cryoprobe's position. When the actual power provided is not exactly the nominal power, the tissue may reach a very different temperature and the thickness of the protected tissue during the cryosurgical procedure will vary accordingly. This analysis provides insight into the sensitivity of the cryoprocedure to errors in the determination of the laser power needed during LAC of prostate cancer.

Acknowledgments

G Aguilar and R Romero-Méndez would like to acknowledge the support of the UC MEXUS programme for a Faculty Fellowship granted to the latter to spend a sabbatical year at UCR. Also, special thanks to Professor John A Viator for proofreading this manuscript.

References

Alexiades V and Solomon A D 1993 *Mathematical Modeling of Melting and Freezing Processes* (Washington, DC: Hemisphere)

Arnott J 1851 *On the Treatment of Cancer by the Regulated Application of an Anaesthetic Temperature* (London: J&A Churchill) p 32

Baissalov R, Sandison G A, Reynolds D and Muldrew K 2001 Simultaneous optimization of cryoprobe placement and thermal protocol for cryosurgery *Phys. Med. Biol.* **46** 1799–814

Chang Z, Finkelstein J J, Ma H and Baust J 1994 Development of a high-performance multiprobe cryosurgical device *Biomed. Instrum. Technol.* **28** 383–90

Çilesiz I and Welch A J 1994 Optical properties of human aorta: are they affected by cryopreservation? *Lasers Surg. Med.* **14** 396–402

Cohen J K, Miller R J and Shuman B A 1995 Urethral warming catheter for use during cryoablation of the prostate *Urology* **45** 861–4

Cohen J K, Miller R, Benoit R, Rooker G and Merlotti L 1998 Five year outcomes of PSA and biopsy following cryosurgery as primary treatment for localized prostate cancer *J. Urol.* **159** 252

Cooper I S and Lee A S 1961 Cryostatic congelation: a system for producing a limited, controlled region of cooling or freezing of biologic tissues *J. Nerv. Ment. Dis.* **133** 259–63

Cooper T E and Trezek G J 1972 Freezing of tissue *J. Heat Trans.* **94** 251–3

Hale G M and Querry M R 1973 Optical constants of water in 200 nm to 200 μm wavelength region *Appl. Opt.* **12** 555–63

Henriques F C 1947 Studies of thermal injury V: the predictability and the significance of thermally induced rate processes leading to irreversible epidermal injury *Arch. Pathol.* **5** 459–502

Hoffmann N E and Bischof J C 2002 The cryobiology of cryosurgical injury *Urology* **60** 40–9

Holistic Urology 2006 The Center of Holistic Urology at the Columbia-Presbyterian Medical Center Website (http://www.holisticurology.columbia.edu/_conditions/prostate_cancer.html)

Incropera F P and DeWitt D P 2002 *Fundamentals of Heat and Mass Transfer* (New York: Wiley)

Lee F, Bahn D K, Badalament R A, Kumar A B, Klionsky D, Onik G M, Chinn D O and Greene C 1999 Cryosurgery for prostate cancer: Improved glandular ablation by use of 6 to 8 cryoprobes *Urology* **54** 135–40

Liu Z H, Wan R, Muldrew K, Sawchuk S and Rewcastle J 2004 A level set variational formulation for coupled phase change/mass transfer problems: application to freezing of biological systems *Finite Elem. Anal. Des.* **40** 1641–63

Mala T, Aurdal L, Frich L, Samset E, Hol P K, Edwin B, Soreide O and Gladhaug I 2004 Liver tumor cryoablation: a commentary on the need of improved procedural monitoring *Technol. Cancer Res. Treat.* **3** 85–91

Onik G M, Cohen J K, Reyes G D, Rubinsky B, Chang Z and Baust J 1993 Transrectal ultrasound-guided percutaneous radical cryosurgical ablation of the prostate *Cancer* **72** 1291–9

Pennes H H 1948 Analysis of tissue and arterial blood temperatures in the resting human forearm *J. Appl. Physiol.* **85** 5–34

Press W H, Flannery B P, Teukolsky S A and Vetterling W T 1986 *Numerical Recipes: The Art of Scientific Computing* (Cambridge: Cambridge University Press)

Rabin Y and Shitzer A 1996 A new cryosurgical device for controlled freezing *Cryobiology* **33** 82–92

Rabin Y and Stahovich T F 2002 The thermal effect of urethral warming during cryosurgery *Cryo Lett.* **23** 361–74

Rabin Y and Stahovich T F 2003 Cryoheater as a means of cryosurgery control *Phys. Med. Biol.* **48** 619–32

Rabin Y, Lung D C and Stahovich T F 2004 Computerized planning of cryosurgery using cryoprobes and cryoheaters *Technol. Cancer Res. Treat.* **3** 229–43

Rees J, Patel B, MacDonagh R and Persad R 2004 Cryosurgery for prostate cancer *BJU Int.* **93** 710–4

Rewcastle J C, Sandison G A, Hahn L J, Saliken J C, McKinnon J G and Donnelly B J 1998 A model for the time-dependent thermal distribution within an iceball surrounding a cryoprobe *Phys. Med. Biol.* **43** 3519–34

Rewcastle J C, Sandison G A, Muldrew K, Saliken J C and Donnelly B J 2001 A model for the time dependent three-dimensional thermal distribution within iceballs surrounding multiple cryoprobes *Med. Phys.* **28** 1125–37

Romero-Mendez R, Chu K, Vu H, Franco W and Aguilar G 2005 Confinement of freezing front by laser irradiation during cryosurgery *Proc. 2004 ASME—Summer Heat Transfer Conference (San Francisco, CA)*

Rubinsky B and Pegg D E 1988 A mathematical-model for the freezing process in biological tissue *Cryobiology* **25** 546

Rubinsky B 2000 Cryosurgery *Ann. Rev. Biom. Eng.* **2** 157–87

Star W M 1995 The relationship between integrating sphere and diffusion-theory calculations of fluence rate at the wall of a spherical cavity *Phys. Med. Biol.* **40** 1–8

Stephenson J 1999 Prostate cancer cryosurgery *JAMA* **282** 226

Warren S G 1984 Optical constants of ice from the ultraviolet to the microwave *Appl. Opt.* **23** 1206–25

Zhu T C *et al* 2005 Optical properties of human prostate at 732 nm measured in mediated photodynamic therapy *Photochem. Photobiol.* **81** 96–105